THE JOURNAL OF PHYSICAL CHEMISTRY C

ARTICLE

pubs.acs.org/JPCC

In Situ ATR-IR Study on the Photocatalytic Decomposition of Amino Acids over Au/TiO_2 and TiO_2

Igor Dolamic[†,‡] and Thomas Bürgi*[,†,§]

[†]Laboratoire de Chimie Physique des Surfaces, Institut de Physique, Université de Neuchâtel, Rue Emile-Argand 11, 2009- Neuchâtel, Switzerland

[§]Physikalisch-Chemisches Institut, Ruprecht-Karls-Universität Heidelberg, Im Neuenheimer Feld 253, 69120 Heidelberg, Germany

ABSTRACT: The photocatalytic degradation of L-asparagine and L-glutamic acid over Au/TiO_2 and TiO_2 catalysts was investigated in situ by attenuated total reflection infrared (ATR-IR) in combination with modulation excitation spectroscopy. Oxalate was detected on the catalyst surface, which has not been reported before for degradation of amino acids by studies focusing on intermediates in solution. The ATR-IR spectra provide valuable information on the fate of the nitrogen. Ammonium was detected, in agreement with previous studies. Most importantly, strong signals of cyanide were observed, and this assignment has been corroborated by ^{15}N labeling experiments. Cyanide was not reported before, to the best of our knowledge, for the photocatalytic degradation of amino acids. Cyanide was formed in the presence and the absence of gold particles on the TiO_2 surface. The cyanide leads to leaching of gold via $Au(CN)_2^-$ species that were detected in solution by mass spectrometry.

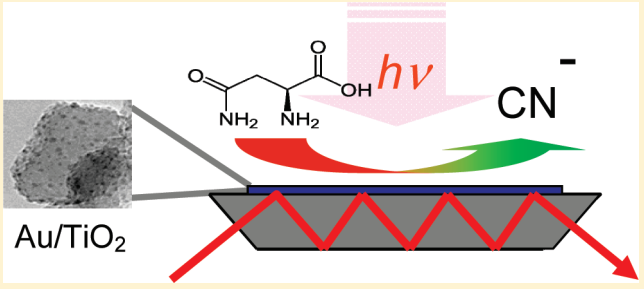

INTRODUCTION

Photocatalysis may play a key role as sustainable technology in the future, for example, in cleaning processes. TiO_2 is a particularly promising photocatalyst because it is chemically inert, has a strong oxidation power, and is cheap. Organic molecules, i.e., pollutants containing C, H, and O, can be mineralized completely to water and CO_2 over TiO_2.[1−4]

An interesting application of photocatalysis by TiO_2-based materials is the inactivation of microorganisms like bacteria, fungi, and single-celled organisms.[5,6] These microorganisms are complex aggregates of different biomolecules. In order to better understand their inactivation under photocatalytic conditions it is beneficial to study the behavior of the individual constituents. Here we focus on the photocatalysis of amino acids over TiO_2-based materials, which has been the subject of several investigations.[7−13]

An important issue in these studies is the fate of the heteroatoms nitrogen and sulfur. We have shown recently that photocatalysis of cysteine derivatives leads to sulfate species.[14] The fate of the nitrogen has been studied for various amino acids. Hidaka and co-workers detected ammonia (NH_4^+) and nitrate (NO_3^-) chromatographically at amount ratios of 3−12 after eight hours reaction time in a batch reactor.[8,15] Horvath and co-workers studied the photodegradation of aspartic acid over bare and silver loaded TiO_2 and found that the nitrogen contained in the amino acid is predominantly converted into NH_3 and after prolonged irradiation into NO_3^-.[13] It was also shown that in the photocatalysis of acetonitrile HCN is formed in the gas[16] and aqueous phases.[17,18]

Photoexcitation of an electron from the valence to the conduction band of TiO_2 leads to the generation of an electron−hole pair. In order to extend the lifetime of the electron−hole pair and to increase the efficiency of the photocatalytic process metal nanoparticles can be deposited onto the TiO_2 semiconductor. The metal particles can act as an electron acceptor,[14,19−21] and therefore, the deposition of metals such as gold, silver, and platinum onto the TiO_2 was considered before by several groups in order to improve the performance of the photocatalysis.[22−32]

Both the electron and the hole can migrate to the surface of the catalyst particle and induce chemical reactions. Photocatalysis by TiO_2 is largely an interface phenomenon. We therefore chose to study the catalytic solid−liquid interface in situ by a combination of attenuated total reflection infrared (ATR-IR) spectroscopy[33−40] and modulation excitation spectroscopy (MES).[41−43] The former technique allows one to measure vibrational spectra of the interface, and the latter provides, among other things, an increased sensitivity. Using this combination of techniques, we show here that on the catalyst surface oxalate is formed as an important intermediate similar as was found for malonic acid degradation.[43] Oxalate was not reported before in studies focusing on the photocatalysis of amino acids probably because it does not desorb into the solution. More importantly we observe strong signals of cyanide (CN^-) in the spectra. Cyanide was not reported before for the photocatalysis of

Received: October 27, 2010
Revised: December 20, 2010
Published: January 14, 2011

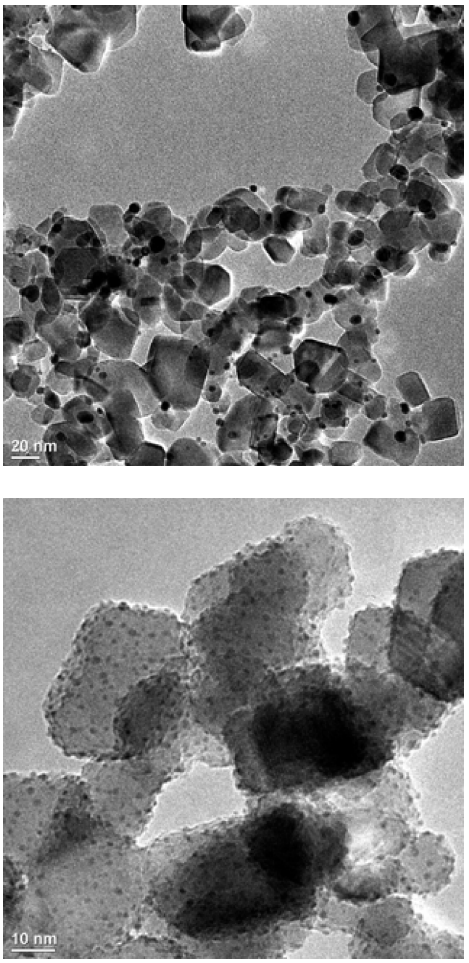

Figure 1. Transmission electron microscopy (TEM) images of NAC-protected gold nanoparticles on TiO_2 before (bottom) and after (top) 2 h of annealing at 300 °C.

amino acids. This finding is relevant in view of the importance of photocatalysis of biological materias.

EXPERIMENTAL SECTION

Catalyst and Chemicals. Commercial type Degussa P25 TiO_2 composed of 80% anatase and 20% rutile with surface area of 51 m^2/g, as given by the supplier, and average particle size of 21 nm was used in the photocatalytic experiments. L-Asparagine (Fluka, 99.5%, L-Asn), L-asparagine-$^{15}N_2$ (ISOTEC 98% ^{15}N), L-glutamic acid (Fluka, 99.5%, L-Glu), L-glutamic ^{15}N acid (Aldrich 98% ^{15}N), KCN (Fluka, ≥98,0%), and HCl (Carlo Erba, 37%) were used as received. Milli-Q (Millipore, 18 MΩ cm) water was used for all experiments.

Preparation of the Au-TiO_2 Catalyst. *N*-Acetyl-L-cysteine monolayer protected gold nanoparticles were prepared as reported previously[44] and were used for the preparation of the gold titanium dioxide catalysts Au-TiO_2. *N*-Acetyl L-cysteine-protected gold nanoparticles (20 mg) of 1−2 nm in core diameter were dissolved in 500 mL of water. The pH of this solution is in the range of 6, which is close to the isoelectric point (IEP) of P25 TiO_2.[45] The aqueous solution of gold nanoparticles was adjusted by addition of 0.1 M HCl to pH = 3.5, and 500 mg of TiO_2 powder was added to the solution. At this pH the surface of TiO_2 is positively charged, which forces the adsorption of the

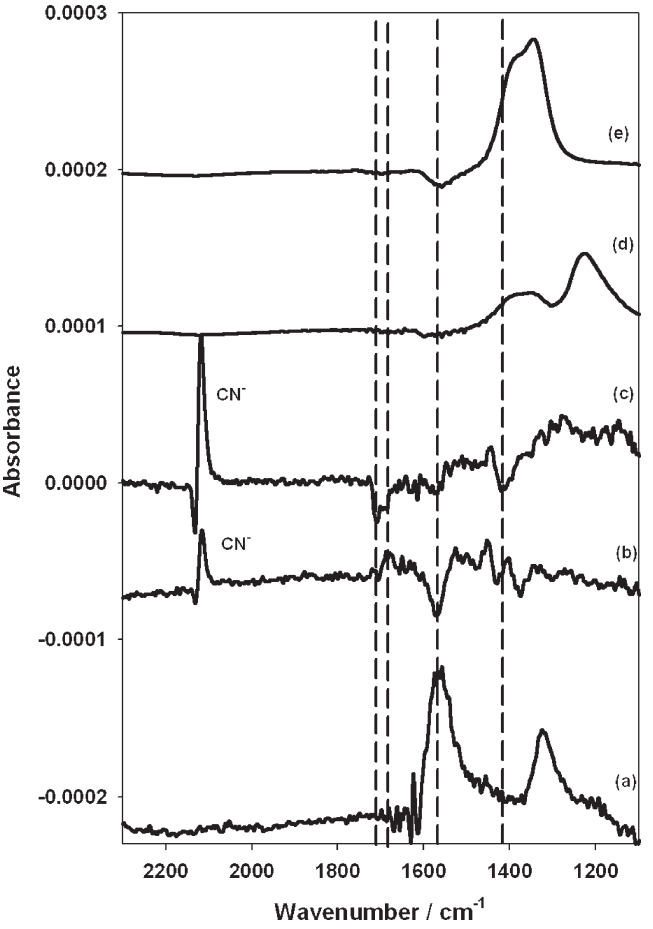

Figure 2. ATR spectra of (a) NH_4Cl, (d) $NaNO_2$, and (e) $NaNO_3$ adsorbed from aqueous solution on Au-TiO_2 and demodulated ATR spectra of a light modulation experiment where solutions of L-glu (1 mM) at pH 5 were flowed over Au-TiO_2 saturated by (b) N_2 and (c) O_2. The concentrations of NH_4Cl, $NaNO_2$, and $NaNO_3$ aqueous solutions were 1 mM. For $NaNO_3$ and NH_4Cl the pH was 3.5, and the pH was 5 for $NaNO_2$. Aqueous solutions of the salts were first flown over the TiO_2 film for 1 h. After adsorption the film was washed with Milli-Q water, leaving (a, d, e) adsorbed species on the surface.

N-acetyl-L-cysteine-protected gold particles. The slurry was stirred for 2 h, filtered off, and washed with water. The catalyst was then heated for 2 h to 300 °C in air. This liberates the *N*-acetyl-L-cysteine from the gold particle surface and leads to a slight increase of the particle size. Figure 1 shows transmission electron microscopy (TEM) images of the Au-TiO_2 catalysts before and after annealing at 300 °C. The size of gold nanoparticles after heating was 5 nm and the gold loading about 2.7 wt %.

Thin films of the catalyst were prepared by suspending 25 mg of Au-TiO_2 catalyst in 25 mL of Milli-Q water. The slurry was sonicated (Branson 200 ultrasonic cleaner) for 30 min. The thin film was formed by dropping the slurry onto a Ge internal reflection element (IRE, 52 mm × 20 mm × 1 mm; KOMLAS). The solvent was evaporated at 30 °C, and the procedure was repeated three times. After drying for several minutes at 30 °C in air, loose catalyst particles were removed by flowing water over the IRE. For every experiment a fresh catalyst film was prepared in the same way.

In Situ Spectroscopy. ATR spectra were recorded with a dedicated flow-through cell, made from a Teflon piece, a fused

dx.doi.org/10.1021/jp1102753 |*J. Phys. Chem. C* 2011, 115, 2228–2234

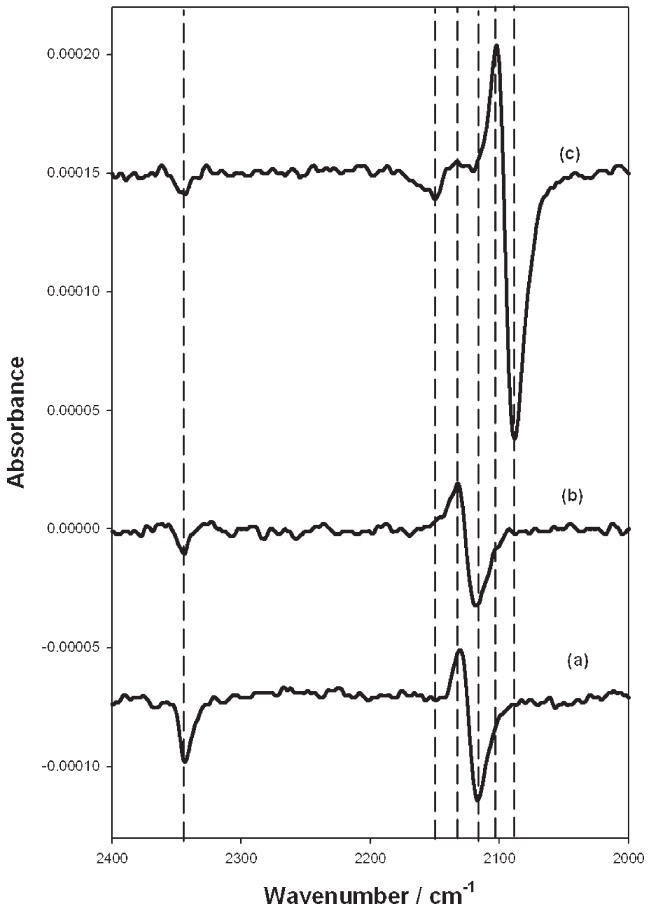

Figure 3. Demodulated ATR spectra of light modulation experiments where aqueous solutions of (a) L-Glu, (b) L-Asn, and (c) $^{15}N_2$-labeled L-Asn at 1 mM concentration and at pH 5 were flowed over Au-TiO_2. The signals slightly above 2100 cm^{-1} belong to the CN stretching vibration of cyanide.

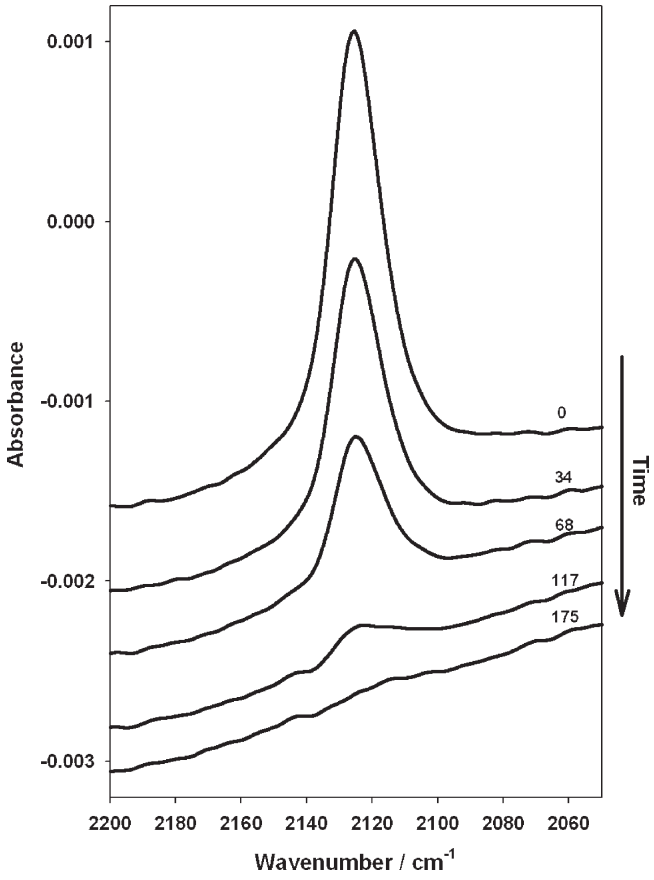

Figure 4. ATR spectra recorded while flowing KCN aqueous solution (1.5×10^{-4} M) over a Au-TiO_2 film. The spectra were recorded (from top to bottom) 0, 34, 68, 117, and 175 s after starting the flow of KCN solution over the film. The signal belongs to the CN stretching vibration of cyanide.

silica plate (45 mm × 35 mm × 3 mm) with holes for in and outlet (36 mm apart), and a flat (1 mm) Viton seal. The cell was mounted on an attachment for ATR measurements within the sample compartment of a Bruker Equinox-55 FTIR spectrometer equipped with a narrow-band MCT detector. Spectra were recorded at 4 cm^{-1}. For irradiation of the sample UV light was provided by a 75 W xenon arc lamp. The UV light from the source was guided to the ATR-IR cell via two fiber bundles. The light was passed through a 5 cm water filter to remove any infrared radiation. Schott UG 11 and BG 42 (50 mm × 50 mm × 1 mm) broadband filters from ITOS were used to remove visible light (transmission between 270 and 380 nm). An estimate based on the supplier specifications gave a power at the sample of slightly less than 2 mW/cm^2.[14]

Electron spray mass spectrometry was used to identify dissolved species. These measurements were performed on an LCQ-IT, Finning instrument equipped with ESI source.

Modulation Excitation Spectroscopy (MES) and Data Acquisition. The catalytic system was stimulated by periodically varying the UV light flux. The concentrations of all species in the system which are affected by this external parameter also change periodically. Phase sensitive detection and subsequent demodulation of the spectra separate the periodical varying from the static signals. By applying MES in combination with ATR-IR spectroscopy, the signal-to-noise ratio can be significantly improved, which assists in the detection of minor species occurring during reaction. During one modulation period (typically 150−235 s), 60 IR spectra were recorded at a sampling rate of 40 or 80 kHz (4−8 scans/s) using the rapid scan function of the FTIR spectrometer. Typically, 20 scans per spectrum recorded in a single period were averaged. Two modulation periods were performed before data acquisition was started. The IR spectra were then averaged over five modulation periods. UV light modulation was achieved using an electronic shutter (Newport model 71445). The light flux was modulated (on−off) in the presence of aqueous amino acid solution over the catalysts. Electrical signals generated by the FTIR spectrometer within the data acquisition loop were used to switch the shutter in order to synchronize modulation and data acquisition. Before the modulation experiments, the amino acid solutions were flowed over the catalysts for 45 min in the dark. After 45 min adsorption equilibrium was reached. The time-resolved absorbance spectra $A = (\tilde{\nu}, t)$ were transformed into phase-resolved spectra using a digital phase sensitive detection (PSD) according to

$$A_k^{\phi_k^{PSD}}(\tilde{\nu}) = \frac{2}{T}\int_0^T A(\tilde{\nu}, t)\sin(k\omega t + \phi_k^{PSD})$$

where $k = 1, 2, 3...$ determines the demodulation frequency (e.g., fundamental, first harmonic), T is the modulation period, $\tilde{\nu}$ denotes the wavenumber, ω the stimulation frequencies and

ϕ_k^{PSD} is the demodulation phase angle. With a set of time-resolved spectra $A = (\tilde{\nu}, t)$ the preceding equation can be evaluated for different demodulation phase angles, ϕ_k^{PSD} resulting in a series of phase-resolved spectra $A_k^{\phi_k^{PSD}}$. More information about the technique can be found elsewhere.[42,46]

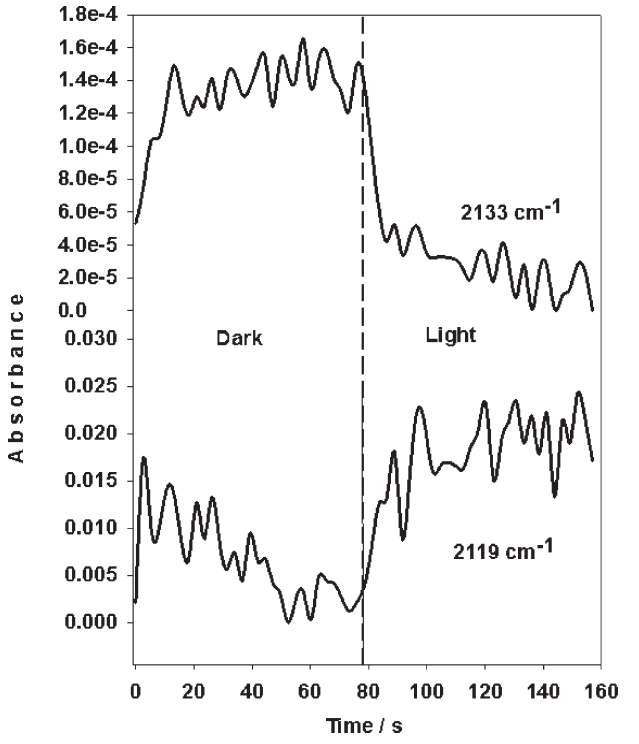

Figure 5. ATR signal as a function of time for a light modulation experiment with modulation period $T = 157$ s. At $T = 0$ the UV light was switched off, and light was switched on at $T = 78.5$ s. The ATR signals were averaged over five modulation periods. The two signals at the indicated wavenumbers are associated with the CN stretching mode.

RESULTS AND DISCUSSION

ATR-IR spectroscopy in combination with modulation spectroscopy shows that during photocatalytic mineralization of amino acids over TiO_2 and Au-TiO_2 film several different species are present on the surface, which is likely related to the complex structure of these molecules. The nature of intermediate species formed upon illumination strongly depends on the reaction conditions, like pH, concentration of dissolved oxygen, and catalyst used. Amino acids can be transformed to oxalate, which is further mineralized to CO_2.[43] Figure 2 shows absorption spectra of NH_4Cl, $NaNO_2$, and $NaNO_3$ aqueous solutions and light modulation experiments under different conditions for the mineralization of L-Glu over Au-TiO_2. When oxygen is present in the experiments, oxalate appears on the surface (spectrum c) giving rise to the bands at 1709 and 1421 cm^{-1}. In contrast, when the reactant solution was saturated by N_2 (spectrum b) oxalate species are suppressed. The dominant broad band at 1567 cm^{-1} in the spectrum is in agreement with the presence of ammonium ions NH_4^+ on Au-TiO_2, which is corroborated by comparison with spectrum a recorded while exposing the Au-TiO_2 catalyst to aqueous NH_4Cl. This is in agreement with a previous report showing that the nitrogen atoms of the amino acids are photoconverted predominantly into NH_4^+ and NO_3^- ions.[8] In the latter work the fate of the nitrogen atom(s) of some amino acids was analyzed using chromatographic methods after about 8 h of illumination. NH_4^+/NO_3^- amount ratios of 3−12 were found. Our experiments indicate the presence of NH_4^+, but no clear sign of NO_3^- (nor NO_2^-) was found (see spectra d and e for comparison). It should be noted, however, that the conditions in the report mentioned above and applied here are different, most

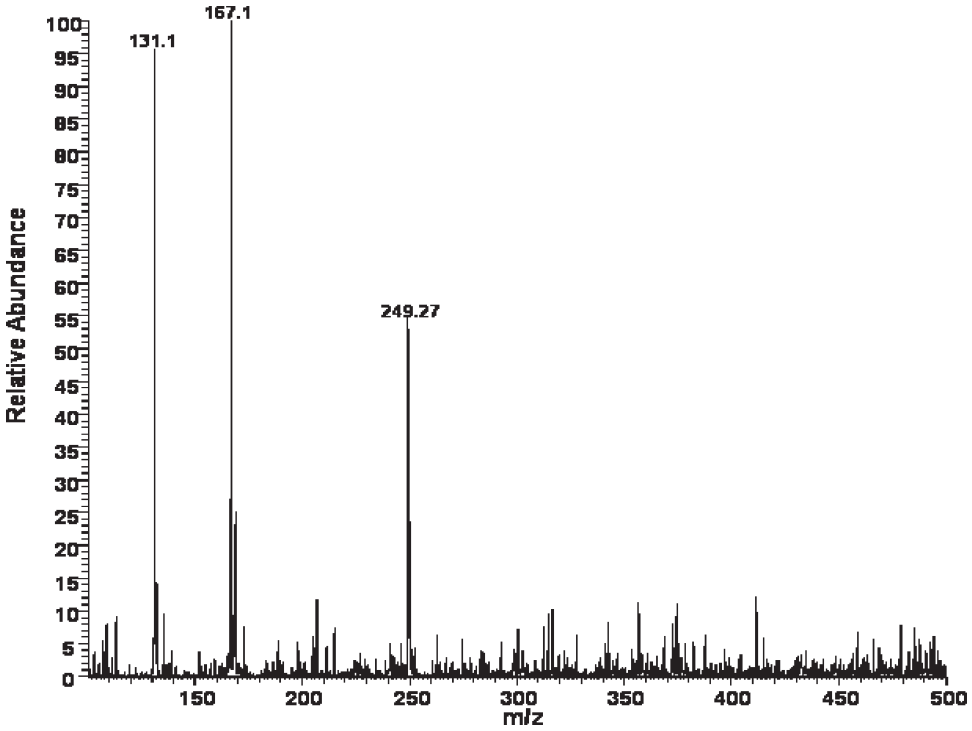

Figure 6. ESI-MS spectrum of cell effluent gathered after photodecomposition of L-asparagine over Au-TiO_2 film in the ATR-IR flow-through cell.

dx.doi.org/10.1021/jp1102753 |J. Phys. Chem. C 2011, 115, 2228–2234

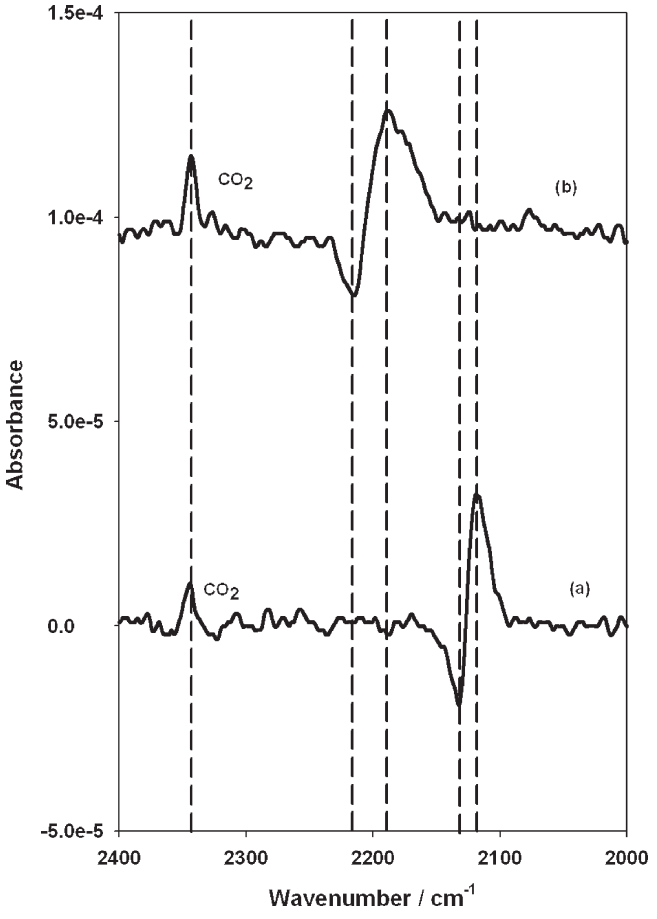

Figure 7. Demodulated ATR spectra of light modulation experiments where L-Asn aqueous solutions (1 mM) at pH 5 were flowed (a) over Au-TiO_2 and (b) over bare TiO_2 film.

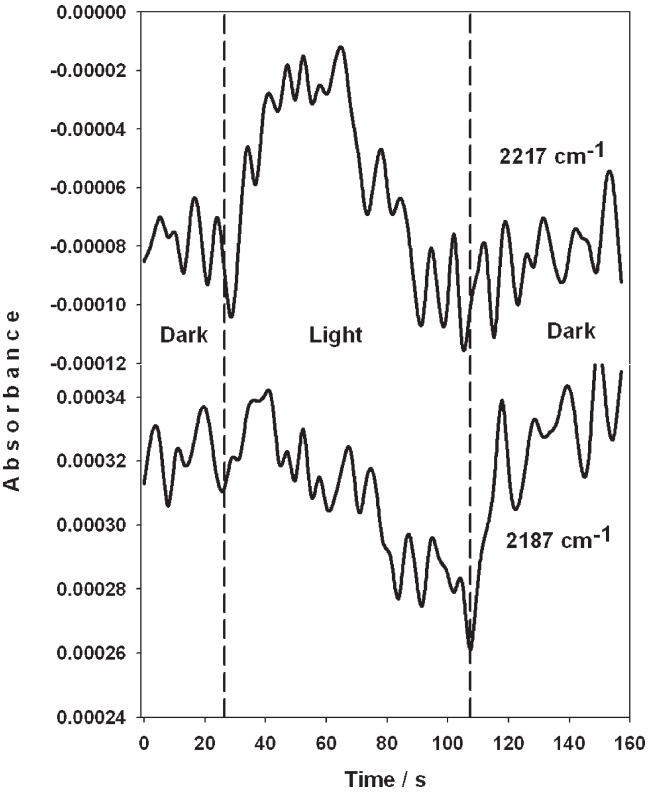

Figure 8. Time dependence of two ATR signals during light modulations experiment with modulation period $T = 157$ s. At $T = 26.1$ s light was switched on and at $T = 104.6$ s switched off. The ATR signals were averaged over five modulation periods. The two signals at the indicated wavenumbers are associated with the CN stretching mode.

importantly the residence time. In our flow-through system the reactant solution is in contact with the catalyst film for some seconds only, whereas eight hours of irradiation in a batch system was used in the work of Hidaka and co-workers.[8] This might indicate that the formation of oxidized species like NO_3^- is a relatively slow process. A study on the photocatalysis of polyvinylpyrrolidine polymer over TiO_2 showed that NH_4^+ is formed immediately whereas NO_3^- was observed only after about 30 min of irradiation.[15] The photocatalytic oxidation of ammonia over TiO_2 and TiO_2 doped with noble metals was reported to yield molecular nitrogen, NO_3^-, and N_2O.[22] In another study it was found that the photocatalytic oxidation of NH_3 to NO_2^-/NO_3^- is the only pathway for decomposition of NH_3 on bare TiO_2, whereas also dinitrogen was found on Pt/TiO_2.[32] In our experiments the most prominent feature in the demodulated ATR-IR spectra both in the presence and absence of dissolved oxygen is a bipolar band at 2133 and 2119 cm^{-1}, which will be discussed in detail in the following part of this work.

Figure 3 shows demodulated spectra of light modulation experiments. In the experiments solutions of (a) L-Glu, (b) L-Asn, and (c) ^{15}N-labeled L-Asn, respectively, at pH = 3.5 were flowed through the ATR-IR cell and over Au-TiO_2 film. The two most prominent bands in spectra a and b are observed at 2133 and 2119 cm^{-1} and will be shown in the following to belong to cyanide CN^- ions adsorbed on the gold nanoparticles. To understand the bipolar nature of the signal (positive, negative) one has to recall that demodulated spectra can be understood as difference spectra between two states. In this case, the two states correspond to light-off and light-on situations. The low energy component at 2119 cm^{-1} is formed during decomposition of the amino acids upon illumination and corresponds to cyanide adsorbed on the gold surface under these conditions. The high energy component at 2133 cm^{-1} belongs to the same species on the gold but in the dark. Spectrum c shows the same species from the experiment where labeled L-Asn was used. Note that all nitrogen atoms are labeled (^{15}N) in L-Asn. The shifts due to the labeling are consistent with CN^-.

The band observed at 2343 cm^{-1} in all experiments is due to dissolved CO_2, which stems from the mineralization of the amino acid. Also, when the CN^- bands shift to lower wavenumbers upon labeling a new band becomes evident in the spectrum at 2157 cm^{-1}. The band may be assigned to CO adsorbed for example on Ti−OH groups. This band position is in good agreement with previous reports.[47] The characteristic band for the Ti_4^+−CO around 2200 cm^{-1} is not observed in our experiments.[48]

To corroborate the identification of the CN^- ions and to learn more about its interaction with the Au-TiO_2 catalyst an aqueous KCN solution (1.5×10^{-4} M) was flowed over the sample. The ATR-IR spectra of this experiment are shown in Figure 4. Right away after starting the flow a band centered at 2125 cm^{-1} becomes evident associated with CN^- adsorbed on gold, in good agreement with the bands observed in the demodulated spectra. However, immediately after that the intensity of the band decreases and completely disappears within around 3 min. This

behavior indicates very fast adsorption of CN^- followed by oxidation of the gold to $Au(CN)_2^-$ and leaching of gold from the TiO_2 surface. Gold cyanidation, i.e., the extraction of gold with cyanide, is a well-known process, which is for example used in gold mining. Indeed, ESI-MS analysis showed the presence of $Au(CN)_2^-$ after admitting KCN to Au-TiO_2 catalyst.

Figure 5 shows the signals at 2133 and 2119 cm^{-1} of CN^- as a function of time during the light modulation experiment of L-Glu. With the light on, the intensity of the band at 2119 cm^{-1} increases, and it decreases when switching the light off again. At the same time the band at 2133 cm^{-1} grows. We ascribe this behavior of the CN^- stretching frequency in the light modulation experiment to the different electronic properties of the catalyst during illumination and in the dark. During illumination photogenerated electrons and holes diffuse to the surface of the TiO_2 particles. Electrons can react with Ti sites according to $e^- + Ti(IV)-O-H \rightarrow Ti(III)-O-H^-$. When illuminating the Au-TiO_2 catalyst the excited electrons from the valence band are accepted by gold nanoparticles due to their high electron affinity and are not (or at least less) trapped at the Ti(IV) sites. Due to the tendency to accept electrons during illumination the potential of the gold particles shifts negative, and this affects the vibrational frequency of CN^- species adsorbed on the metal surface.[49] From the wavenumber shift the potential change of gold nanoparticles can be estimated to around 0.4 V.[49]

Figure 5 also shows that the bands at 2133 and 2119 cm^{-1} show different kinetics for the appearance and disappearances. In the dark and during illumination the properties of the gold particles are different due to the different potential. When the gold particles are electron rich, the potential is negative and the coverage of the adsorbed CN^- increases. When the gold particles become neutral, the coverage of adsorbed CN^- species decreases upon oxidation of gold. The time-resolved spectra (not shown) reveal that CN^- species are present on the surface during both experimental states, i.e., in the dark and during illumination.

The presence of the CN^- species on the Au-TiO_2 catalyst, as spectroscopically observed, may imply leaching of the gold nanoparticles from the TiO_2 support and formation of $AuCN_2^-$ complexes in the solution. Figure 6 shows the ESI-MS spectrum of the cell effluent gathered for a photocatalytic experiment where L-Asn was decomposed over Au-TiO_2. During that experiment L-Asn was adsorbed in the dark on the Au-TiO_2 catalyst. Reaching adsorption equilibrium the UV light was switched on and a sample was collected at the ATR cell outlet for 10 min. The ions at 131 and 167 m/z are assigned as $[L\text{-Asn} - H]^-$ and $[L\text{-Asn} - H + 2H_2O]^-$, respectively, corresponding to unreacted L-Asn. The ion at 249.27 m/z assigned as $[Au(CN)_2]^-$ can be related to the process of gold leaching during degradation of amino acid over Au-TiO_2.

Figure 7 shows demodulated spectra of light modulation experiments. In these experiments a solution of L-Asn was flowed over bare TiO_2 (spectrum b) and Au-TiO_2 catalyst (spectrum a). From spectrum b it is clear that CN^- species are formed on the TiO_2 surface as well. Also, in both spectra dissolved carbon dioxide is observed.[43] Figure 8 shows the time dependence of the two signals at 2217 and 2187 cm^{-1} on TiO_2 during the experimental course. When the system is illuminated the band at 2217 cm^{-1} is formed very fast on the surface reaching maximum in 65 s and after that vanishes quickly reaching a minimum after around 90 s. This behavior of the band implies that CN^- intermediates are formed on the TiO_2 catalyst and destroyed during irradiation as well. The band at 2187 cm^{-1} develops in intensity when the light is off. This band can be assigned to adsorbed cyanide on TiO_2 (Ti−CN) that was not destroyed during the irradiation process on the TiO_2 surface.[50] The band at 2217 cm^{-1} is assigned to (Ti−NCO) species that formed during oxidation of cyanide on the surface.[50] Bard and coworkers reported oxidation of cyanide over TiO_2 and formation of OCN^- species.[51,52] This shows that CN^- is oxidized over bare TiO_2 catalyst upon illumination. By comparison of the spectra in Figure 7 it can be concluded that on the Au-TiO_2 the CN^- adsorbs on the gold, since no sign of CN^- on TiO_2 is evident. This reveals the much larger affinity of CN^- for gold than for TiO_2.

CONCLUSIONS

Our in situ ATR-IR experiments show that in the presence of oxygen in solution oxalate species can be observed on the TiO_2 surface during the photocatalytic mineralization of amino acids over Au-TiO_2 and TiO_2. The experiments furthermore shed some light on the fate of the nitrogen atom. Ammonium and particularly cyanide were observed. The latter species was not reported before for the photocatalytic degradation of amino acids. This finding is relevant in view of the application of photocatalysis to biological materials. Moreover, in the case of the Au-TiO_2 the cyanide leads to the leaching of gold in the form of $[Au(CN)_2]^-$ which can be detected in solution. In contrast, cyanide that was formed on bare TiO_2 led to the formation of OCN^- species on the TiO_2 surface. A shift of the vibrational frequency of CN^- adsorbed on the gold particles is observed upon illumination. This shift is attributed to the transfer of photogenerated electrons from the conduction band of TiO_2 to the gold particles. This shifts the electrochemical potential of the gold, which in turn influences the CN stretching frequency. ATR-IR spectroscopy therefore offers the possibility to determine these important potential shifts on the metal particles in situ.

AUTHOR INFORMATION

Corresponding Author

*E-mail: buergi@uni-heidelberg.de.

Present Addresses

‡Institute of Inorganic Chemistry, University of Zürich, Winterthurerstrasse 190, CH-8057 Zürich, Switzerland.

REFERENCES

(1) Asahi, R.; Morikawa, T.; Ohwaki, T.; Aoki, K.; Taga, Y. *Science* **2001**, *293*, 269.
(2) Hoffmann, M. R.; Martin, S. T.; Choi, W. Y.; Bahnemann, D. W. *Chem. Rev.* **1995**, *95*, 69.
(3) Linsebigler, A. L.; Lu, G. Q.; Yates, J. T. *Chem. Rev.* **1995**, *95*, 735.
(4) Hashimoto, K.; Irie, H.; Fujishima, A. *Jpn. J. Appl. Phys., Part 1* **2005**, *44*, 8269.
(5) Wolfrum, E. J.; Huang, J.; Blake, D. M.; Maness, P. C.; Huang, Z.; Fiest, J.; Jacoby, W. A. *Environ. Sci. Technol.* **2002**, *36*, 3412.
(6) Zheng, H.; Maness, P. C.; Blake, D. M.; Wolfrum, E. J.; Smolinski, S. L.; Jacoby, W. A. *J. Photochem. Photobiol., A* **2000**, *130*, 163.
(7) Martra, G.; Horikoshi, S.; Anpo, M.; Coluccia, S.; Hidaka, H. *Res. Chem. Intermed.* **2002**, *28*, 359.
(8) Hidaka, H.; Horikoshi, S.; Ajisaka, K.; Zhao, J.; Serpone, N. *J. Photochem. Photobiol., A* **1997**, *108*, 197.
(9) Hidaka, H.; Ajisaka, K.; Horikoshi, S.; Oyama, T.; Zhao, J. C.; Serpone, N. *Catal. Lett.* **1999**, *60*, 95.

(10) Ikeda, S.; Sugiyama, N.; Pal, B.; Marci, G.; Palmisano, L.; Noguchi, H.; Uosaki, K.; Ohtani, B. *Phys. Chem. Chem. Phys.* **2001**, *3*, 267.
(11) Hidaka, H.; Shimura, T.; Ajisaka, K.; Horikoshi, S.; Zhao, J. C.; Serpone, N. *J. Photochem. Photobiol., A* **1997**, *109*, 165.
(12) Matsushita, M.; Tran, T. H.; Nosaka, A. Y.; Nosaka, Y. *Catal. Today* **2007**, *120*, 240.
(13) Szabo-Bardos, E.; Petervari, E.; El-Zein, V.; Horvath, A. *J. Photochem. Photobiol., A* **2006**, *184*, 221.
(14) Dolamic, I.; Gautier, C.; Boudon, J.; Shalkevich, N.; Burgi, T. *J. Phys. Chem. C* **2008**, *112*, 5816.
(15) Horikoshi, S.; Hidaka, H.; Serpone, N. *J. Photochem. Photobiol., A* **2001**, *138*, 69.
(16) Krichevskaya, M.; Joks, S.; Kachina, A.; Preis, S. *Photochem. Photobiol. Sci.* **2009**, *8*, 600.
(17) Addamo, M.; Augugliaro, V.; Coluccia, S.; Di Paola, A.; Garcia-Lopez, E.; Loddo, V.; Marci, G.; Martra, G.; Palmisano, L. *Int. J. Photoenergy* **2006**, 12.
(18) Addamo, M.; Augugliaro, V.; Coluccia, S.; Faga, M. G.; Garcia-Lopez, E.; Loddo, V.; Marci, G.; Martra, G.; Palmisano, L. *J. Catal.* **2005**, *235*, 209.
(19) Dawson, A. *J. Phys. Chem. B* **2001**, *105*, 960.
(20) Subramanian, V.; Wolf, E. E.; Kamat, P. V. *J. Am. Chem. Soc.* **2004**, *126*, 4943.
(21) Carneiro, J. T.; Savenije, T. J.; Mul, G. *Phys. Chem. Chem. Phys.* **2009**, *11*, 2708.
(22) Kolinko, P. A.; Kozlov, D. V. *Appl. Catal., B* **2009**, *90*, 126.
(23) Ismail, A. A.; Bahnemann, D. W.; Bannat, I.; Wark, M. *J. Phys. Chem. C* **2009**, *113*, 7429.
(24) Bannat, I.; Wessels, K.; Oekermann, T.; Rathousky, J.; Bahnemann, D.; Wark, M. *Chem. Mater.* **2009**, *21*, 1645.
(25) Min, B. K.; Heo, J. E.; Youn, N. K.; Joo, O. S.; Lee, H.; Kim, J. H.; Kim, H. S. *Catal. Commun.* **2009**, *10*, 712.
(26) Petrov, L.; Iliev, V.; Eliyas, A.; Tomova, D.; Puma, G. L. *J. Environ. Prot. Ecol.* **2007**, *8*, 881.
(27) Paramasivalm, I.; Macak, J. M.; Schmuki, P. *Electrochem. Commun.* **2008**, *10*, 71.
(28) Orlov, A.; Chan, M. S.; Jefferson, D. A.; Zhou, D.; Lynch, R. J.; Lambert, R. M. *Environ. Technol.* **2006**, *27*, 747.
(29) Sakthivel, S.; Shankar, M. V.; Palanichamy, M.; Arabindoo, B.; Bahnemann, D. W.; Murugesan, V. *Water Res.* **2004**, *38*, 3001.
(30) Arabatzis, I. M.; Stergiopoulos, T.; Andreeva, D.; Kitova, S.; Neophytides, S. G.; Falaras, P. *J. Catal.* **2003**, *220*, 127.
(31) Subramanian, V.; Wolf, E. E.; Kamat, P. V. *Langmuir* **2003**, *19*, 469.
(32) Lee, J.; Park, H.; Choi, W. *Environ. Sci. Technol.* **2002**, *36*, 5462.
(33) Connor, P. A.; Dobson, K. D.; McQuillan, A. J. *Langmuir* **1999**, *15*, 2402.
(34) Hug, S. J.; Sulzberger, B. *Langmuir* **1994**, *10*, 3587.
(35) Dolamic, I.; Burgi, T. *J. Phys. Chem. B* **2006**, *110*, 14898.
(36) Bürgi, T.; Baiker, A. *Adv. Catal.* **2006**, *50*, 227.
(37) Ortiz-Hernandez, I.; Williams, C. T. *Langmuir* **2003**, *19*, 2956.
(38) Ebbesen, S. D.; Mojet, B. L.; Lefferts, L. *J. Catal.* **2007**, *246*, 66.
(39) Almeida, A. R.; Moulijn, J. A.; Mul, G. *J. Phys. Chem. C* **2008**, *112*, 1552.
(40) Ferri, D.; Burgi, T.; Baiker, A. *J. Phys. Chem. B* **2001**, *105*, 3187.
(41) Baurecht, D.; Fringeli, U. P. *Rev. Sci. Instrum.* **2001**, *72*, 3782.
(42) Burgi, T.; Baiker, A. *J. Phys. Chem. B* **2002**, *106*, 10649.
(43) Dolamic, I.; Burgi, T. *J. Catal.* **2007**, *248*, 268.
(44) Gautier, C.; Burgi, T. *Chem. Commun.* **2005**, 5393.
(45) Gumy, D.; Morais, C.; Bowen, P.; Pulgarin, C.; Giraldo, S.; Hajdu, R.; Kiwi, J. *Appl. Catal., B* **2006**, *63*, 76.
(46) Urakawa, A.; Wirz, R.; Burgi, T.; Baiker, A. *J. Phys. Chem. B* **2003**, *107*, 13061.
(47) Toledo-Antonio, J. A.; Capula, S.; Cortes-Jacome, M. A.; Angeles-Chavez, C.; Lopez-Salinas, E.; Ferrat, G.; Navarrete, J.; Escobar, J. *J. Phys. Chem. C* **2007**, *111*, 10799.
(48) Hadjiivanov, K.; Lamotte, J.; Lavalley, J. C. *Langmuir* **1997**, *13*, 3374.
(49) LeRille, A.; Tadjeddine, A.; Zheng, W. Q.; Peremans, A. *Chem. Phys. Lett.* **1997**, *271*, 95.
(50) Rasko, J.; Bansagi, T.; Solymosi, F. *Phys. Chem. Chem. Phys.* **2002**, *4*, 3509.
(51) Frank, S. N.; Bard, A. J. *J. Am. Chem. Soc.* **1977**, *99*, 303.
(52) Frank, S. N.; Bard, A. J. *J. Phys. Chem.* **1977**, *81*, 1484.